Reprinted from Coastal Upwelling
Coastal and Estuarine Sciences 1

PHYSICAL AND BIOLOGICAL STRUCTURE AND VARIABILITY IN AN UPWELLING CENTER OFF PERU NEAR 15°S DURING MARCH, 1977

K.H. Brink

School of Oceanography, Oregon State University, Corvallis, Oregon 97331

B.H. Jones *

Bigelow Laboratory for Ocean Sciences, West Boothbay Harbor, Maine 04575

J.C. Van Leer

Division of Physical Oceanography, Rosenstiel School of Marine and Atmospheric Sciences, University of Miami, Miami, Florida 33149

C.N.K. Mooers

Department of Oceanography, Naval Postgraduate School, Monterey, California 93940

D.W. Stuart

Department of Meteorology, Florida State University, Tallahassee, Florida 32306

M.R. Stevenson

Instituto de Pesquisas Espaciais (INPE)
Caixa Postal 515, São José dos Campos - S.P. 12,200, BRAZIL

R.C. Dugdale

Institute of Marine and Coastal Studies, University of Southern California, University Park, Los Angeles, California 90007

G.W. Heburn

Department of Meteorology, Florida State University, Tallahassee, Florida 32306

* Present Address: Department of Biological Sciences, Allan Hancock Foundation, University of Southern California, Los Angeles, California 90007

Abstract. The upwelling region near 15°S off Peru was studied intensively during the period 12 to 30 March 1977. A surface cold area (apparent "plume") is a persistent feature of the region, and it has an associated biological signature. Horizontally, the cold water generally extended equatorward and offshore from the coast; vertically, the alongshore structure was 40% as strong at 40 m depth as at the surface, and imperceptible at 64 m. The size of the surface cold area increased as the local alongshore wind stress increased. Physical variability was also dependent

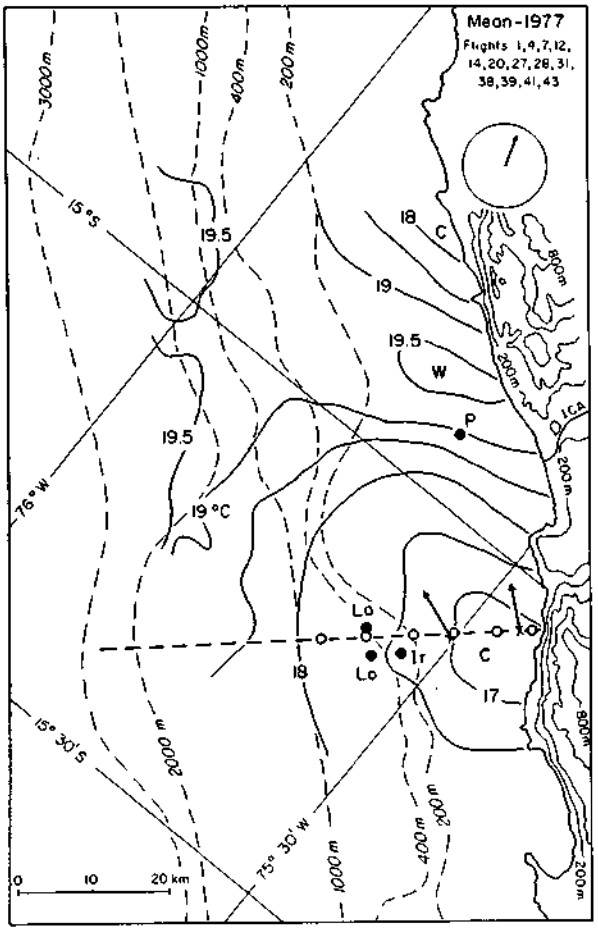

Fig. 1. Mean sea-surface temperature from 13 ART flights between March 21 and May 6, 1977. Plate III can be used to place this figure in a larger scale context. The heavy dashed line represents the C line, and the open circles denote the standard C stations: C-1 (closest to shore), out to C-6. The arrows represent the mean 4.5-m velocity vectors at PSS-Agave (closer to shore) and at PS-Mila. The length of the arrow is the distance that the flow would traverse in 12 h_2. The circle in the upper right hand corner contains the mean wind stress vector, and the radius of the circle is 1 dyne/cm . Symbols representing other current meter moorings: P = Parodia, La = Lagarta, Lo = Lobivia, Ir = Ironwood.

upon the passage of coastally trapped waves. Biological variability and structure were closely related to the physical regime. Physical and biological aspects of wind-driven upwelling events are described, and the biological dynamics of the upwelling center are discussed.

Introduction

The distribution of sea-surface temperature along the coast of Peru is far from uniform. As a region of persistent upwelling-favorable winds, it would be expected to have a band of cold, nutrient-rich water nearshore with progressively warmer, nutrient-depleted waters farther offshore. While this general pattern does obtain, there is comparably important alongshore variation in sea-surface temperature, with alternating warm and cold patches (Zuta, Rivera, and Bustamante, 1978). In particular, near 15°S, there is a cold patch previously described by Ryther *et al.* (1966), by Eber, Saur, and Sette (1968), and by Smith, Enfield, Hopkins, and Pillsbury (1971). The hydrographic and airborne radiometric measurements obtained throughout the CUEA (Coastal Upwelling Ecosystems Analysis) JOINT-II experiment of 1977 also confirm the existence of a surface cold spot, or horizontal plume, which generally had its origin at the same location on the coast (Fig. 1). The feature appeared to strengthen, deform, and decay as the local wind stress fluctuated in time. The coldest water of the patch, 16 to 18°C, was usually at the coast near 15° 05.5'S, 75°24'W, and spread about 50 km seaward and equatorward. Higher surface nutrient concentrations and biological productivity with low phytoplankton biomass are associated with the cold area (Walsh, Kelley, Dugdale, and Frost, 1971).

The upwelling center, representing both physical and biological phenomena, is perhaps best investigated by an interdisciplinary approach. Even for an approximate description of the physical regime, a combination of measurements is needed. The biological problem requires even greater breadth because nutrients, phytoplankton, and higher trophic levels interact in a highly variable, spatially complex physical environment. In the following, we shall attempt to describe the upwelling center through an integration of physical and biological observations. Ambiguities in description will arise because of the considerable temporal and spatial variability inherent to the system.

The Upwelling Center Study

The present study attempts a synthesis of several kinds of observations with the goal of jointly describing the physical, chemical, and biological regimes. The data were taken over a roughly 40 by 60-km region off the Peru coast near 15°S (Fig. 1), and the period of the study is an 18-day subset (12-30 March, 1977) of the 14-month JOINT-II program. This particular period was chosen for closer study because of the unusually intensive data acquisition at the time. Four ships were in the area, two conducting physical (drogue and synoptic-scale hydrographic) observations, and two primarily conducting biological, hydrographic, and chemical observations. Methods used in the drogue studies are described by Stevenson, Garvine, and Wyatt (1974) and by Stevenson (1974), while the synoptic-scale hydrography is described by Johnson, Koeb, and Mooers (1979). Details of the biological and large-

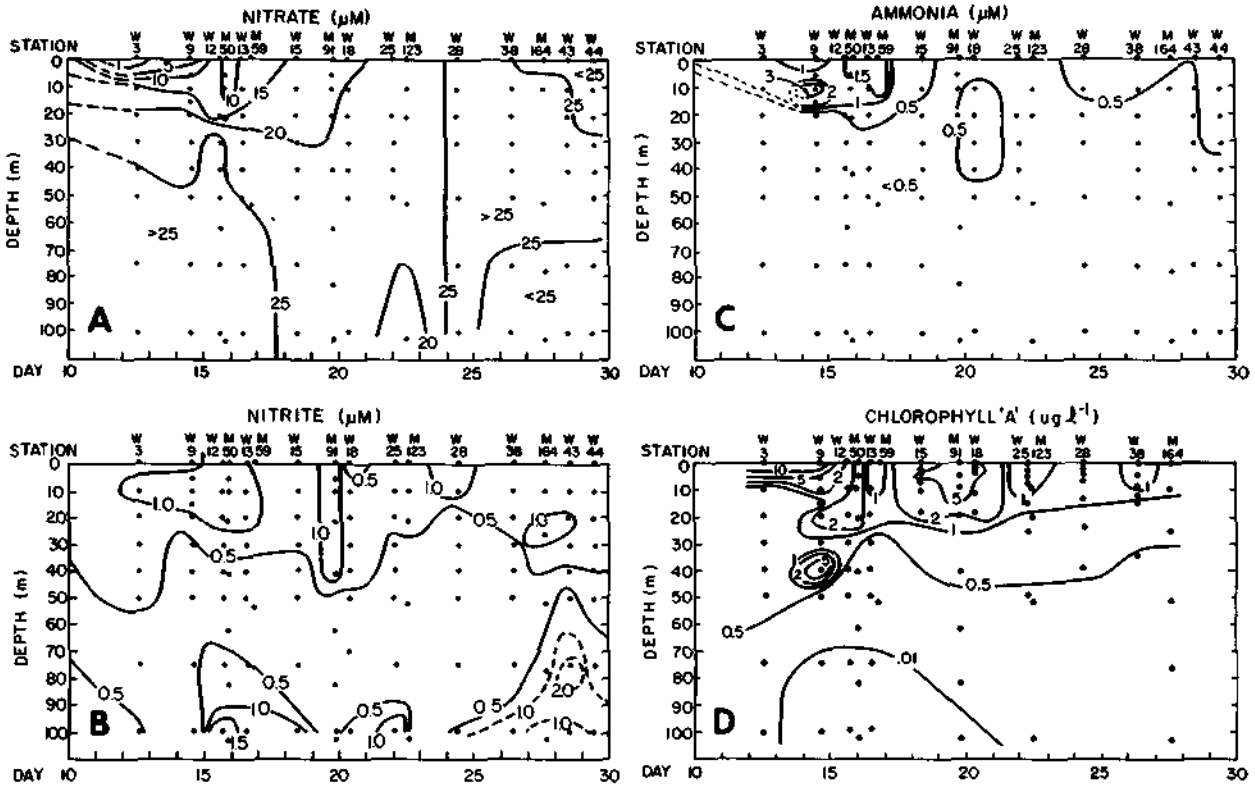

Fig. 2. Contour plots of chemical variables at the mid-shelf (C-3) position.

scale hydrographic studies can be found in Kogelschatz, MacIsaac, and Breitner (1980) and in Hafferty, Codispoti, and Huyer (1978). Also during the period, four airborne radiometric surface temperature (ART) charts were made at about noon local time (see Moody, 1979). In addition, fixed-point observations were made, including an array of 40 current meters, four Cyclosonde profiling current meters, and three meteorological buoys (Brink, Halpern, and Smith, 1980; Van Leer and Ross, 1979). Land-based observations included wind, solar radiation, and sea level (Moody, 1979; Brink *et al.*, 1980).

In the following, all wind and current time series are resolved into cross-shelf (positive for shoreward flow) and alongshore (positive for equatorward flow) components. The rotation angle of the coordinate system was 45° counterclockwise from true north, consistent with the general trend of the coastline. Over the shelf, this choice of coordinate system agrees to ± 2.5° with the depth-averaged principal axis system used at each mooring by Brink *et al.* (1980). Throughout the following, only the wind stress record from mooring PSS, about 4 km from shore on the central mooring line, will be used. To synchronize with the times of aircraft flights, most time series data discussed are treated with a 12-h running mean, centered on 0500 and 1700 GMT. Following J.J. O'Brien (personal communication), the vertical velocity was estimated from current meter data at a position at 20 m depth roughly midway between the PSS current meter (Fig. 1) and the coast. The position was chosen because it is the estimated site of the most intense upwelling.

Most of the hydrographic data were observed along the C line, a line normal to the coast and passing through the area of low mean surface temperature. Stations along the line are denoted by C-1, C-2, etc., with the number increasing with distance from the coast. A time series of biological and chemical variables was sampled daily (Fig. 2) at the mid-shelf (C-3) position, near the most heavily instrumented current meter mooring.

The Mean Upwelling Center

Physical Observations

Throughout the March to May 1977 period, and in particular during our study period, the local alongshore winds were equatorward, hence favorable for upwelling (Fig. 3). Means of other physical variables over the 18-day period are also representative of longer term measurements (Brink *et al.*, 1980). The wind stress forced a pattern in cross-shelf velocity that was qualitatively con-

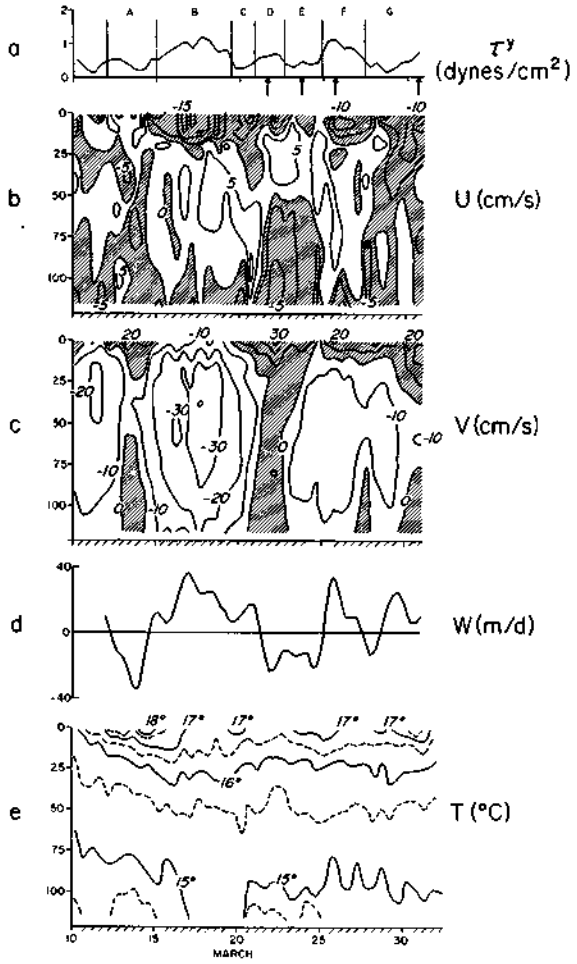

Fig. 3. Physical measurements at mid-shelf: a) alongshore wind stress at PSS, τ^y (dyne/cm^2); b) cross-shelf velocity (cm/s). Negative (shaded) values correspond to offshore flow; c) alongshore velocity (cm/s). Positive (shaded) values correspond to equatorward flow; d) estimated vertical velocity (m/d) at 20-m depth, 2 km from shore (J.J. O'Brien, personal communication). Positive values correspond to upward motion. e) Tempera ture (°C). Panels b), 3), and e) were drawn from observations at depths 2.1, 4.6, 8.1, 12, 16, 20, 24, 39, 59, 80, 100, and 115 m.

sistent with Ekman upwelling dynamics at the mid-shelf C-line position (Fig. 4). Brink *et al.* (1980) demonstrated that the mean onshore transport is in approximate agreement with two-dimensional Ekman theory, but the offshore transport is about one-third that predicted by theory. The result implies a strong alongshore variability in the near-surface flow pattern associated with the upwelling circulation. The mean noon-time ART chart (Fig. 1) shows that there is considerable alongshore thermal structure, consistent with the presence of alongshore structure in the velocity field.

The mean (over 14 nightly CTD transects) temperature along the C-line section (Fig. 5a) has a relatively strong surface gradient (baroclinic zone) 10 to 25 km off the coast. The gradient marks the outer limits of the cool surface area evident in the ART charts. The companion salinity section (Fig. 5b) has a nearshore minimum apparently due to alongshore advection of the Ica River plume, as confirmed by visual observations of color from an aircraft. The low salinity water reduces nearshore density to the point where the mean σ_t = 25.6 isopycnal outcrops (Fig. 5c). The density structure below the upper 20 m is consistent, through a thermal wind bal-

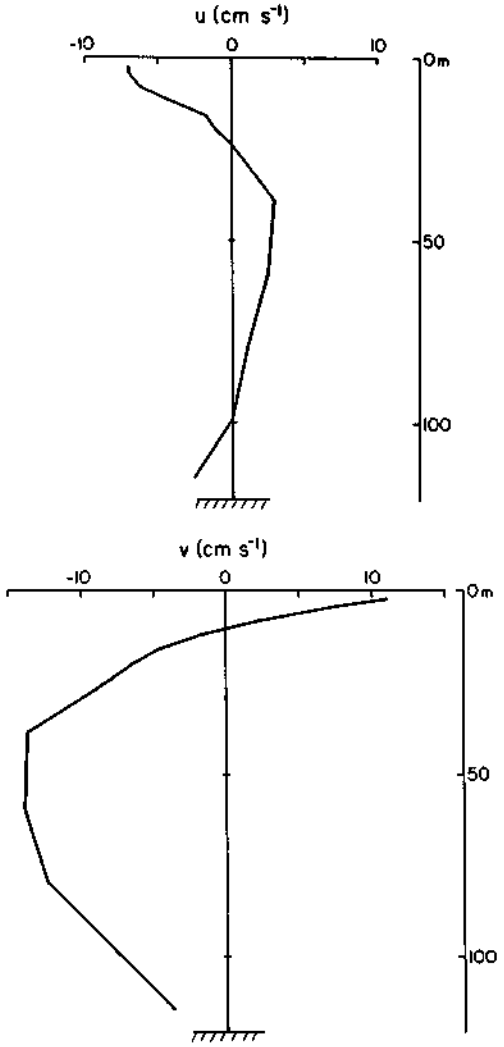

Fig. 4. Mean velocity components at the mid-shelf (PS-Mila) position, March 12 to 30, 1977. The cross-shelf component, u, is positive for onshore flow, and the alongshore component, v, is positive for equatorward flow.

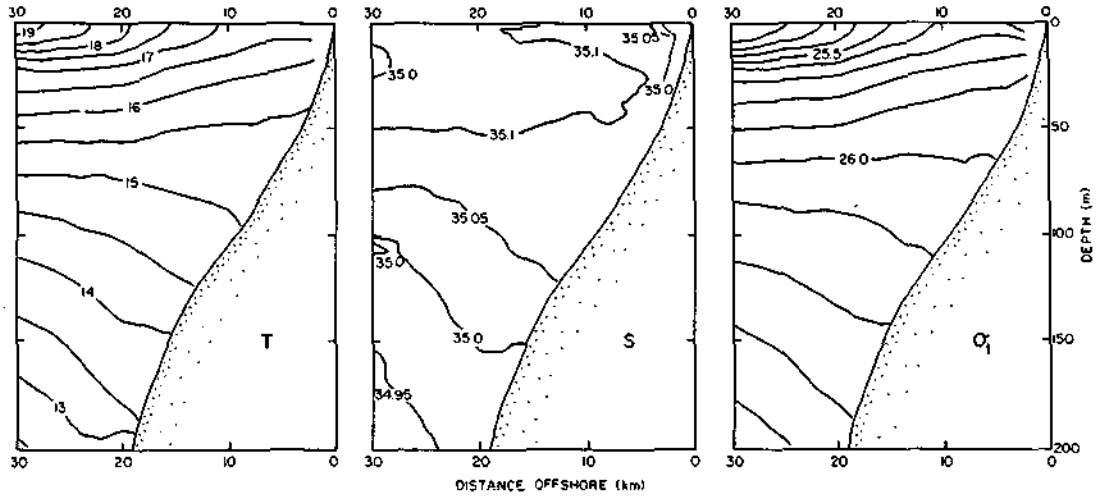

Fig. 5. Mean CTD hydrography along the C line from 14 nightly sections, March 16 to 30, 1977.

ance, with the observed mean alongshore currents, i.e., equatorward near-surface currents overlying a poleward undercurrent, which had its maximum mean speed at about mid-depth over the entire shelf.

Current measurements at fixed locations, cross-shelf hydrographic transects, and sea-surface temperature charts, however, give only a partial picture of the physical nature of the upwelling center. How deep did the structure observed at the surface penetrate? Because the mid-shelf mean onshore transport (below roughly 25 m) fits a two-dimensional model, the surface structure probably did not extend significantly below 25 m. Data derived from mid-shelf moored instrumentation (i.e., at Parodia and C-3) show that the mean alongshore temperature gradient, a measure of the structure's intensity, decreased considerably with depth; the mean gradients were 2.2 x 10^{-2}°C/km at 3 m, 0.8 x 10^{-2}°C/km at 24 m, and indistinguishable from zero at 64 m. The figures suggest that the alongshore structure disappeared by about 50-m depth on average, a notion supported by a CTD survey during our study period (Fig. 6).

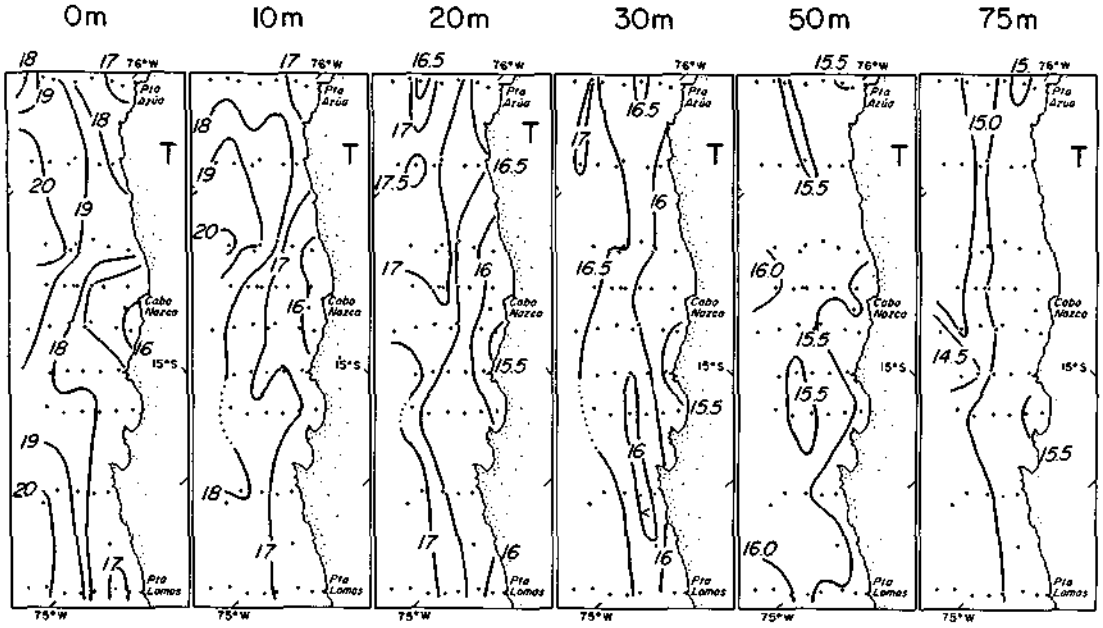

Fig. 6a. Ship-based mapping results, March 20–23, 1977. Temperature (°C) at depths 0, 10, 20, 30, 50, and 75 m (from Huyer and Gilbert, 1979).

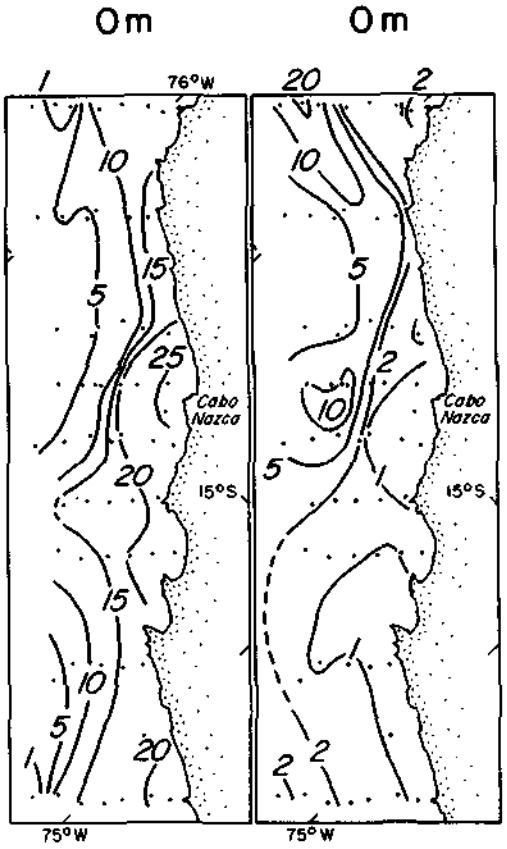

Fig. 6b. Ship-based mapping results, March 20-23, 1977. Surface nitrate (μM) and chlorophyll *a* (μg/l).

The overall structure and dynamics of the near-surface flow field are also poorly resolved. The mean wind is not uniform in space (Brink, Smith, and Halpern, 1978); it was strongest at position PSS (near shore on the C line), and weakened both farther offshore (C-3) and with alongshore distance from the C line. Unlike the winds, however, the mean 4.5-m velocities were stronger at C-3 and directed more nearly offshore than at PSS. Near-surface drogue data (Figs 7, 8, and 9) suggest a tendency for cross-isotherm (i.e., radially outward) flow, although the data are too few to be conclusive. To the extent that frontal dynamics (e.g., Mooers, Collins, and Smith, 1976) applied, a geostrophic component of flow was superimposed on the directly wind driven component. Order-of-magnitude estimates (Brink *et al.*, 1980) support this hypothesis for the mean flow. Frontal dynamics also imply the presence of a further small-scale frictional component in the flow. The mean surface temperature map (Fig. 1) shows no sharp fronts, as they tend to average out due to their variability in position and intensity. Individual maps, however, do occasionally show sharp frontal features (Figs 7 and 8), which also are clearly evident in some cross-shelf profiles of aircraft sea-surface temperature (e.g., Stuart and Bates, 1977).

Chemical and Biological Observations

Average C-line sections of chemical variables were computed using 14 transects occupied between March 5 and May 16, 1977 (Fig. 10). The longer time period was chosen to obtain a more stable mean than would have been obtained from the four chemical sections occupied during the interval discussed in this study. We feel that the shorter period is sufficiently representative that the use of the longer-term mean is reasonable (compare Figs 10, 11, 12, 13, 14).

The nitrite maximum-nitrate minimum was a persistent feature offshore, centered at about 200 m (Fig. 10a and 10b; see also Hafferty, Lowman, and Codispoti, 1979). The contour lines, 20 μM for

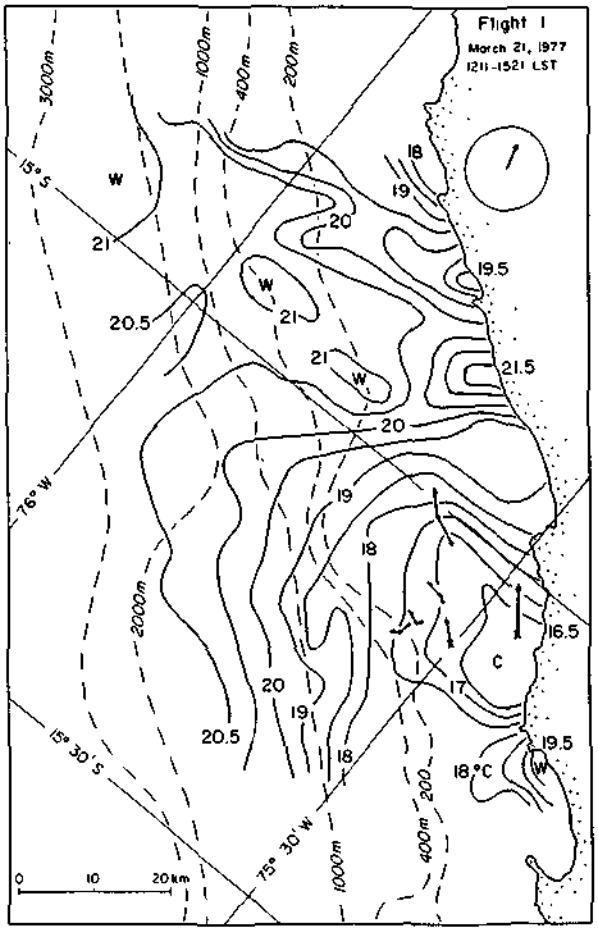

Fig. 7a. Sea-surface temperature (°C) from an aircraft flight near noon local time on March 21, 1977. Conventions for wind stress and velocity are given with Fig. 1.

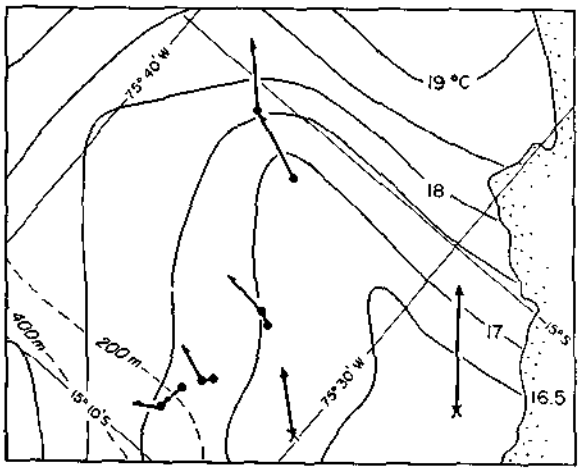

Fig. 7b. The displacement of 4-m drogues over 12 h centered on the aircraft flight near noon local time on March 21, 1977.

NO_3 and 1 μM for NO_2, both extend up over the shelf near the bottom indicating that some of the nitrite-rich – nitrate-poor water was frequently present on the shelf. A subsurface core of high nitrate (>24 μM) water was present at about 25 m near the coast and increased in depth to about 50 m at 30 km offshore (C-6). The mean surface nitrate concentration was essentially constant between 1 and 7 km offshore, this being the apparent region where most of the upwelling was occurring (Brink *et al.*, 1980). The surface nitrate concentration then decreased in the offshore direction but remained higher than 5 μM out to 50 km.

Silica (Fig. 10c), unlike nitrate, increased monotonically with depth. Near-bottom silicate concentrations of greater than 30 μM extended over the shelf to the most inshore station. Near-surface silica concentrations declined monotonically in the offshore direction. Nitrate and silica were about the same concentration nearshore, and silica was only slightly less concentrated than nitrate 30 km offshore.

Chlorophyll *a* (Fig. 10d) was low nearshore and increased to a maximum in the region of strong mean cross-shelf temperature gradient, about 18 km offshore. For a region known for its high primary productivity and the resultant high phytoplankton biomass, the values (∿3 μg/l) appear to be anomalously low. A year earlier in this area, concentrations had been 25 to 30 μg/l and even higher when dense *Gymnodinium splendens* blooms were present (Dugdale *et al.*, 1977; Jones, 1977). Also, during *Anton Bruun* cruise 15 in 1966 (Ryther *et al.*, 1966) and during the PISCO cruise in 1969 (Walsh *et al.*, 1971), near-surface chlorophyll *a* concentrations coincident with the 17.5°C isotherm were approximately 10 μg/l. Finally, Barber (1981) showed that, for reasons that are not understood, the area-averaged chlorophyll *a* levels in this vicinity were lower in 197; than in 1966, 1976, or 1978.

The Variability

To explore the coupled physical and biological variability, events are discussed chronologically through the period of detailed observations. For convenience, the 18-day period is broken up into sub-sections defined primarily by the local alongshore wind stress, hence the strength of local coastal upwelling. The sub-sections are designated alphabetically (Fig. 3). A more general discussion with conclusions on time variability will follow the chronological description.

The major forms of physical variability can readily be isolated from the data. One is wind driven, which includes mixed-layer deepening and offshore Ekman transport, the clearest signatures of which are in the distribution of temperature and of onshore velocity (Brink *et al.*, 1980). The

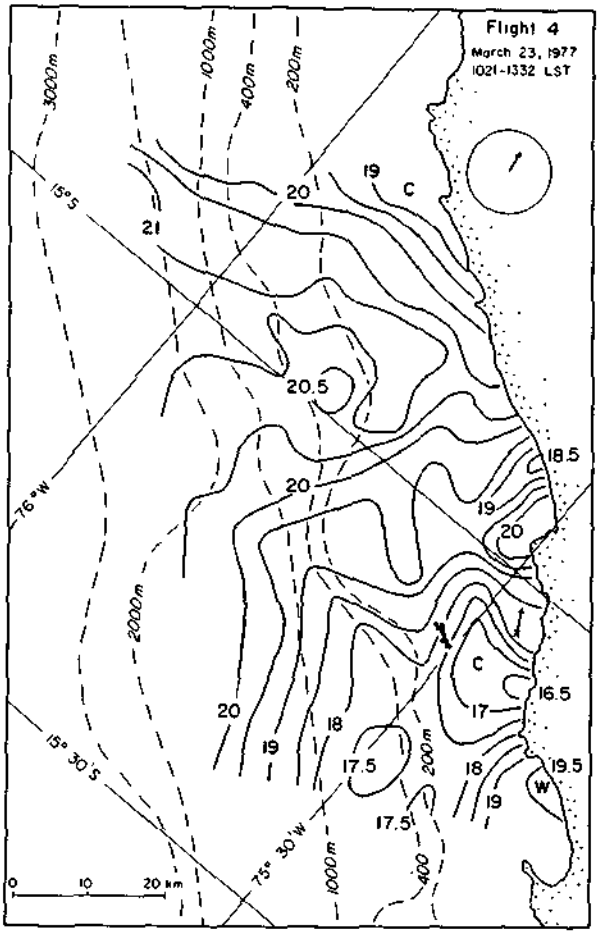

Fig. 8a. Sea-surface temperature (°C) from an aircraft flight near noon local time on March 23, 1977. Conventions are the same as in Fig. 7. Drogues were set to 4-m depth.

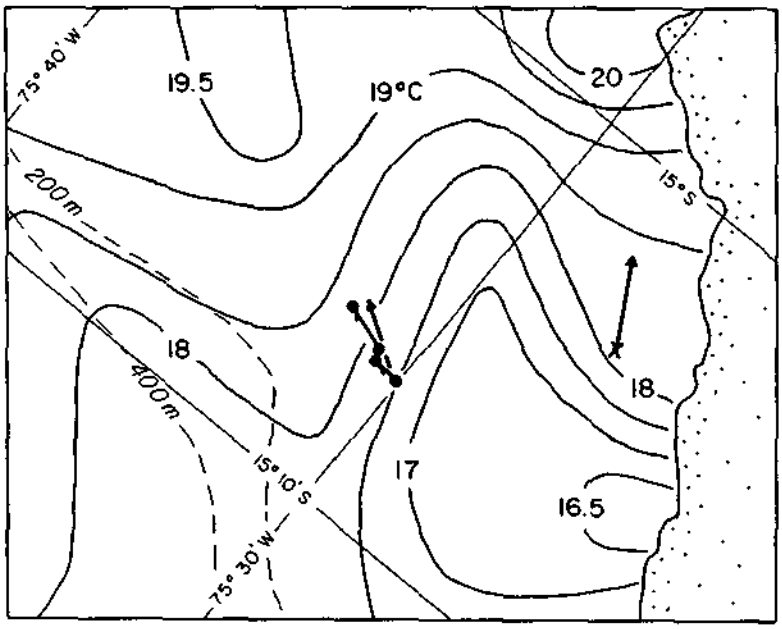

Fig. 8b. Sea-surface temperature (°C) from an aircraft flight near noon local time on March 23, 1977. Conventions are the same as in Fig. 7. Drogues were set to 4-m depth.

second major form of physical variability is related to free coastally trapped waves, which dominate the alongshore velocity fluctuations. The origin of the waves is not fully known, but they are baroclinic in nature (i.e., velocity fluctuations are associated with density fluctuations) and they propagate poleward at about 200 km/d (Smith, 1978; Brink *et al.*, 1980). In the following, the forms of physical variability will be described in conjunction with chemical and biological variability.

Period A: Weak Winds

During a period (March 12 to 14) of weak, though equatorward, winds, the estimated nearshore vertical velocities ranged from weakly upward to strongly downward (Fig. 3) and the surface mixed layer at mid-shelf was thin or nonexistent (Fig. 15). The onshore flow over the shelf was relatively disorganized. The mid-shelf near-surface water can be classified as "old" in the sense that phytoplankton biomass was relatively high (Fig. 2d) and nitrate (Fig. 2a) and other primary nutrients were depleted, presumably due to consumption by the phytoplankton. Near-surface nitrite (Fig. 2b) and ammonia (Fig. 2c) were high and presumably byproducts of phytoplankton consumption (Estrada and Wagensberg, 1977) and of zooplankton grazing (Smith and Whitledge, 1977). On March 15, at the end of the quiet phase, a hydrographic section showed a distinct maximum in chlorophyll *a* at the surface near the shelf break, about 20 km from shore (Fig. 11). Near-surface nitrate concentrations decreased gradually from relatively high values near shore to very low values more than 23 km offshore. An upwelling response was beginning, as evidenced by offshore near-surface flow, onshore currents below, and upwarped isotherms in the upper 50 m over the shelf.

Period B: Strong Upwelling

From 15 to 19 March, a strong wind-driven upwelling event was superimposed on a very intense coastally trapped wave. The onshore-offshore current structure (Figs 3 and 12) clearly showed the effects of the upwelling event: strong offshore flow in the upper 20 m, onshore flow greater than 5 cm/s over most of the remainder of the water column, and nearshore vertical velocities estimated to be as large as 36 m/day. The mid-shelf surface mixed layer had a deepening trend during this time (Fig. 15). The warm, nitrate-poor near-surface water had been advected farther offshore and replaced by waters richer in nitrate (Fig. 12). The mid-shelf waters (Fig. 2) were lower in both primary and secondary products of phytoplankton productivity: chlorophyll *a*, nitrite, and ammonia. The near-surface shelf-break chlorophyll *a* maximum remained at the same position as on March 15 (Fig. 12) but had grown considerably stronger.

Coincident with the wind event was the passage of a strong coastally trapped wave, which had passed Callao, near 12°S, two days earlier, producing a period of strong (velocities as large as 40 cm/s) poleward current (Brink *et al.*, 1978). The wave caused poleward flow throughout the mid-

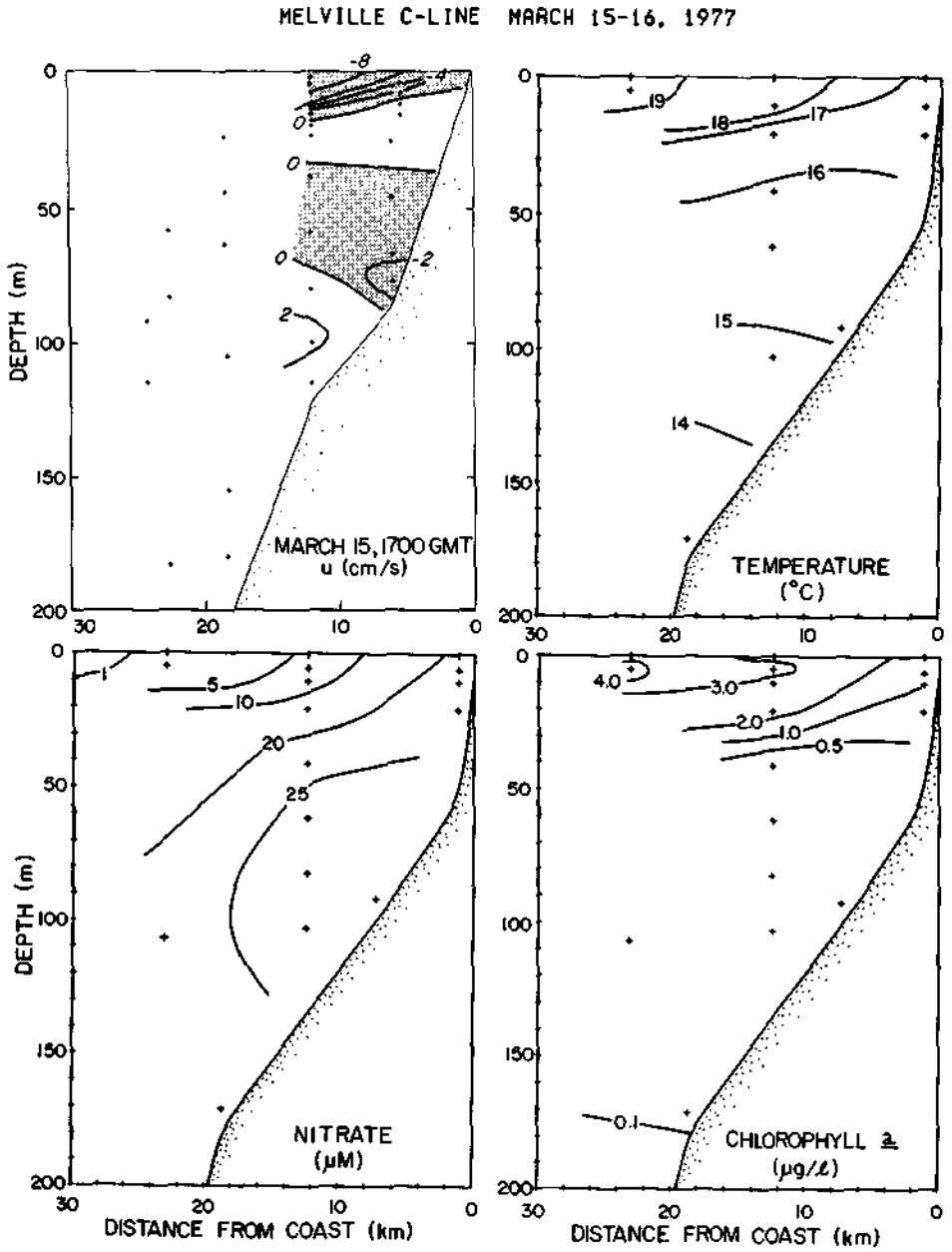

Fig. 11. Hydrographic section of March 15, 1977. Upper left, onshore velocity (cm/s). Negative values correspond to offshore flow.

tory. The events of March 15 to 19 suggest that although structures can change and new effects can be introduced by the coastally trapped wave's passage, upwelling processes continued despite the wave's presence, and immediate effects on the surface layer primary productivity were not apparent.

Period C: Weak Winds

During a brief period (March 19 and 20) of weak winds, the poleward alongshore flow associated with the coastally trapped wave decreased and the upwelling circulation remained detectable in the cross-shelf flow (Fig. 3). The mid-shelf

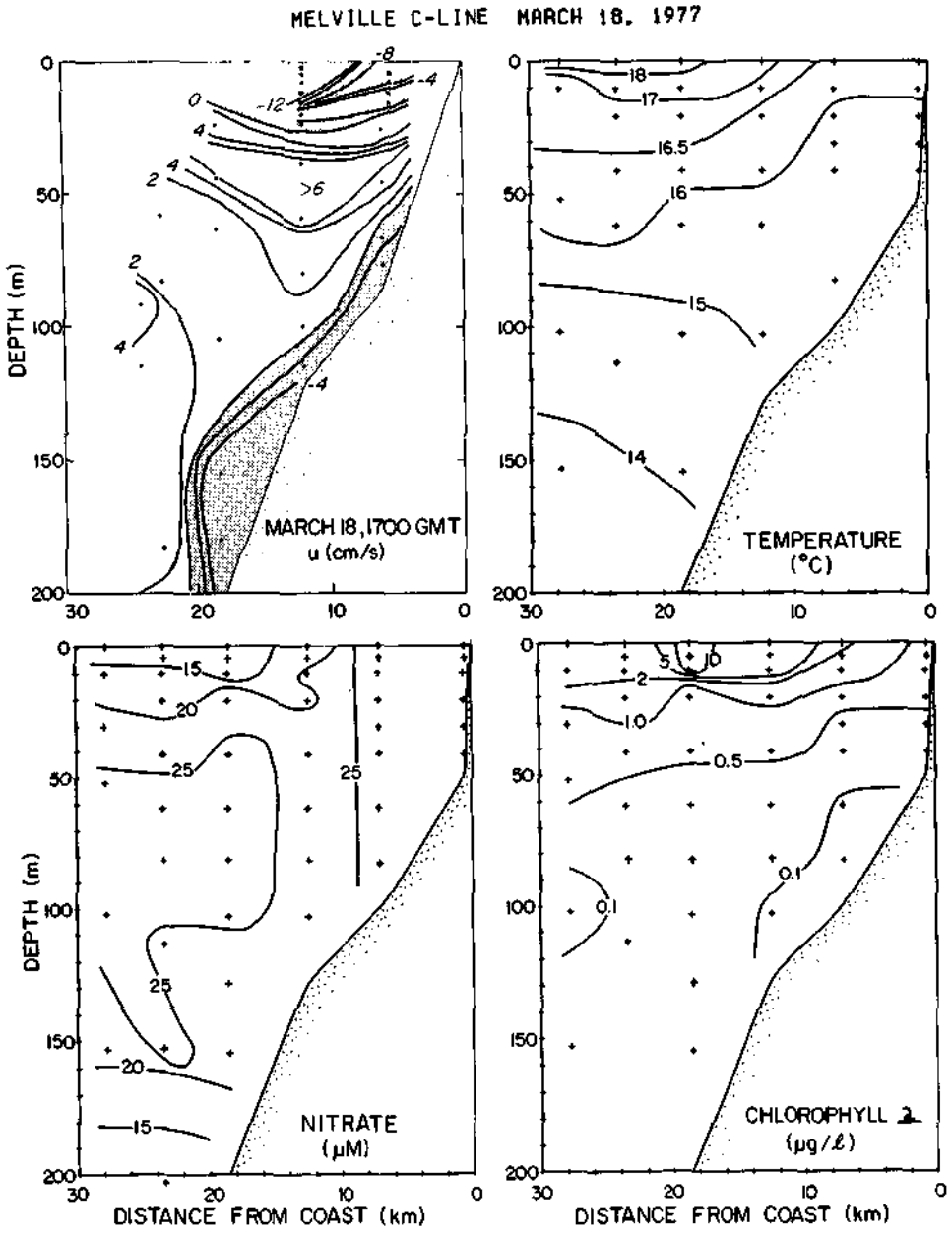

Fig. 12. Hydrographic section of March 18-19, 1977. Sections are the same as in Fig. 11.

near-surface waters warmed by an amount consistent with estimated surface heating (estimates show that solar radiation is generally the dominant surface heat flux), and the mid-shelf surface-mixed layer became thin or non-existent (Fig. 15). Shallow chlorophyll *a* also increased during the period (Fig. 2), indicating phytoplankton growth. This overall pattern appears to be typical of relaxation following an upwelling event.

Period D: Shallow Upwelling

Centered on March 21, a brief, weak wind event occurred. Coincident with the event and with the passage of a coastally trapped wave there was equatorward flow throughout the water column over the shelf. The flow structure could act to break down the phytoplankton reseeding as did the poleward flow during March 15 to 19. There appeared to be upwelling associated with the wind event,

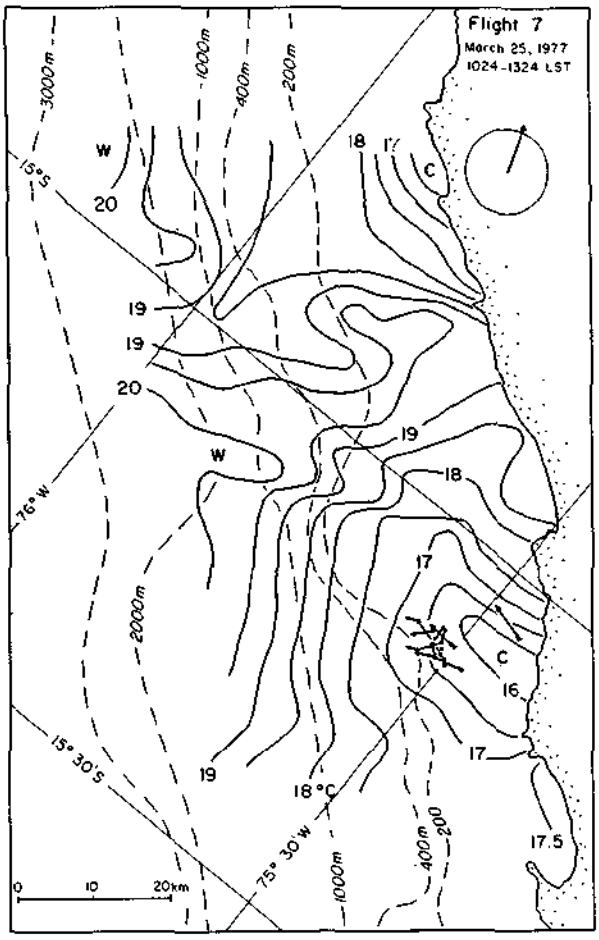

Fig. 9a. Sea-surface temperature (^{o}C) from an aircraft flight near noon local time on March 25, 1977. Conventions are as in Fig. 7. Drogues were set to 4-m depth.

shelf (C-3) water column (Fig. 3), despite the strong (greater than 1 dyne/cm^2) equatorward wind stress. Associated with the wave, through the thermal wind balance, isotherms in the depth range of 80 to 250 m tilted downward toward the coast (Fig. 12). For example, the 15^{o} isotherm was displaced downward and seaward of C-3 for three days (Fig. 3). During the wave passage, nitrite values were relatively high as much as 50 m above the bottom (Fig. 2). Normally, enhanced nitrite was found only relatively close (within about 10 m) to the shelf bottom (Fig. 10a), apparently as a result of regeneration in the sediments or in the near-bottom waters. During the wave passage, unusually high speeds resulting in strong near-bottom shears apparently caused a significant increase of the bottom boundary layer thickness (Fig. 16). Thickening of the bottom mixed layer presumably allowed near-bottom water to penetrate higher into the water column.

This particular wave passage seems to have had considerable delayed biological consequences. Under mean conditions, an upwelled phytoplankter would be initially advected equatorward and offshore. As the individual sinks at a rate of, say, 10 m/d (Smayda, 1970) it would, after about two days, settle into a subsurface region of onshore and poleward currents. Thus, there is a tendency for phytoplankton to return to the general region of origin. Allowing for grazing, turbulent dispersion, and the time and spatial variability of the flow, it appears that at least some small fraction will generally be returned to the upwelling center, providing a phytoplankton inoculum to the upwelled water. This idea, treated two-dimensionally by Smith and Barber (1980), is supported by the high water-column averaged chlorophyl (1 μg/l) at position C-1. If the alongshore flow for some period is in the same direction throughout the water column, the reseeding mechanism can break down, because the settled phytoplankton would be upwelled at some considerable distance alongshore from their origin. As the coastally trapped wave caused poleward flow over the entire shelf, the phytoplankton stock normally associated with the upwelling center was apparently advected away. Thus, during the next upwelling event, waters from roughly 40 to 120 km equatorward would be upwelled, and they could have a considerably lower phytoplankton content (provided they came from a less productive region).

Biological observations following a 4-m (a depth well within the near-surface layer defined by PS onshore velocity; Fig. 3) drogue began on March 18 at C-3. The drogue and those launched at about the same time (at other depths) moved

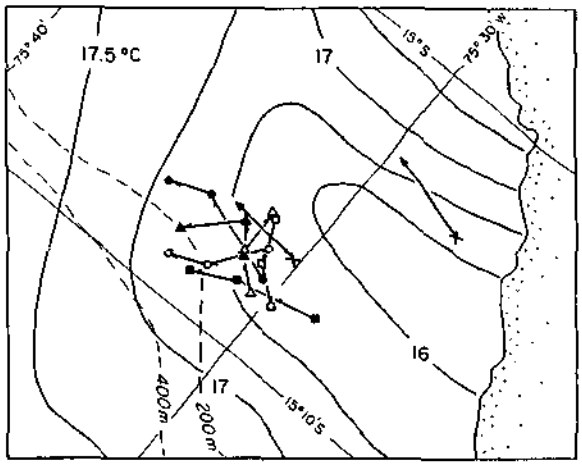

Fig. 9b. Sea-surface temperature (^{o}C) from an aircraft flight near noon local time on March 25, 1977. Conventions are as in Fig. 7. Drogues were set to 4-m depth.

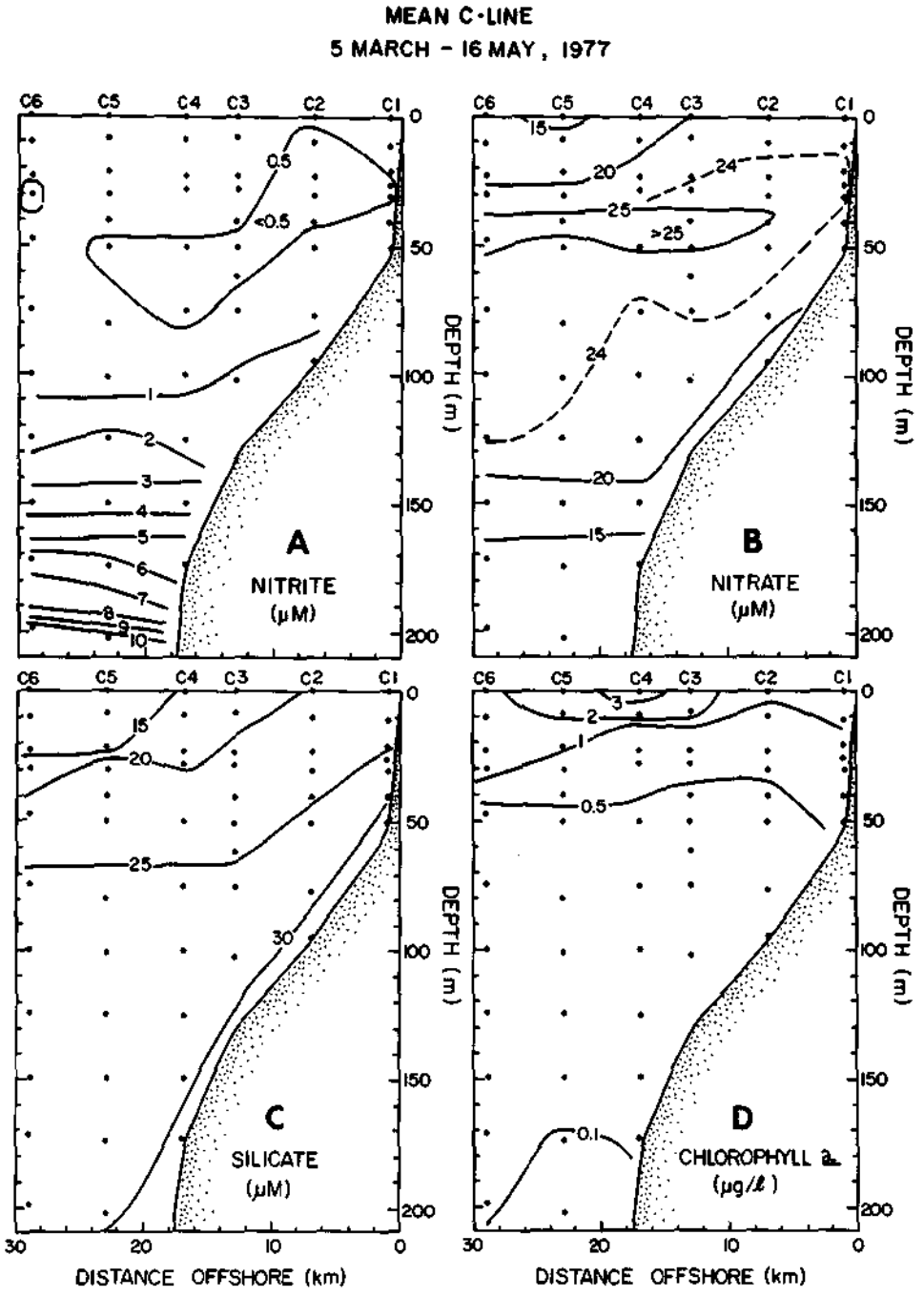

Fig. 10. Mean chemical C line, averaged over sections made between March 5 and May 6, 1977.

poleward initially (Fig. 17a), consistent with the dominance of the wave-associated poleward velocities throughout the mid-shelf water column (Fig. 3). On March 19, after the passage of the wave, the 4-m drogue moved generally offshore and equatorward, consistent with the return to dominance of wind-driven effects on alongshore currents at this depth. Near-surface biological measurements were made daily at the drogue's location and show a sequence of "aging" of freshly upwelled water (Fig. 17b): temperature, chlorophyll *a*, and nitrite increase monotonically, while nitrate, other nutrients, and nitrogen uptake rates decreased along the drogue's trajec-

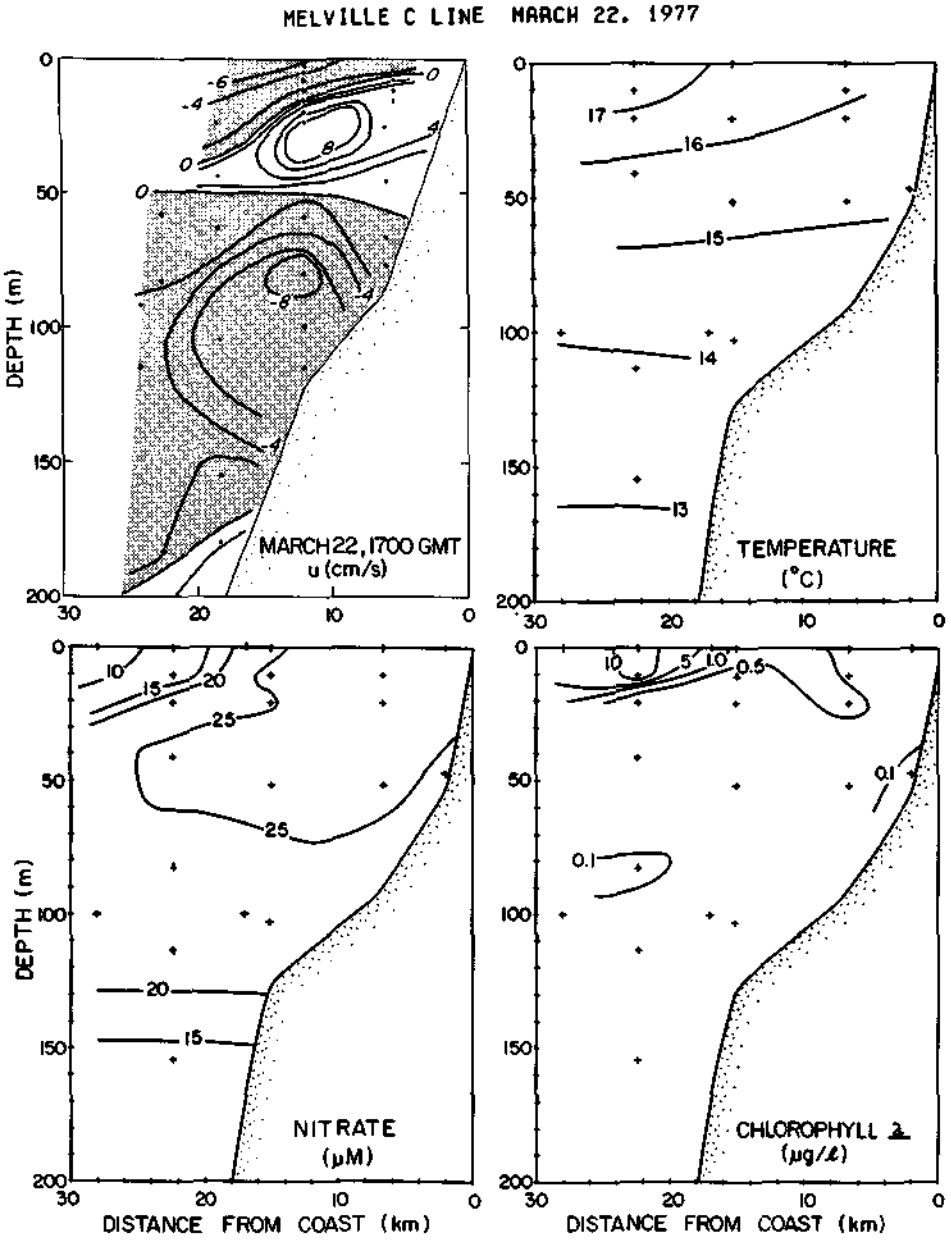

Fig. 13. Hydrographic section of March 22, 1977. Upper left, onshore velocity (cm/s). Sections as in Fig. 11.

with onshore flow between 15 and 50 m (Fig. 3). The mid-shelf surface mixed layer deepened to as much as 16 m during the event (Fig. 15). The near-surface flow at mid-shelf was strongly offshore in the upper 15 m, but nearshore, at PSS, the flow was onshore, so that estimated vertical velocities show the apparent upwelling only initially. The near-surface flow on March 21 was divergent and there was a large cold spot (<16.5°C) centered at the coast slightly south of the C line (Fig. 7). The structure was present to 30 to 50-m depth (Fig. 6a). The near-surface drogues at the time moved outward from the center of the cold area, suggesting a region of divergent flow. The axis of the cold area was directed equatorward from directly offshore, consistent with the near-surface northward flow. About 40 km north of the cold spot there was a distinct warm patch (>21.5°C). The strong alongshore variation in surface temperature is indicative of an accompanying alongshore structure in the upwelling circulation.

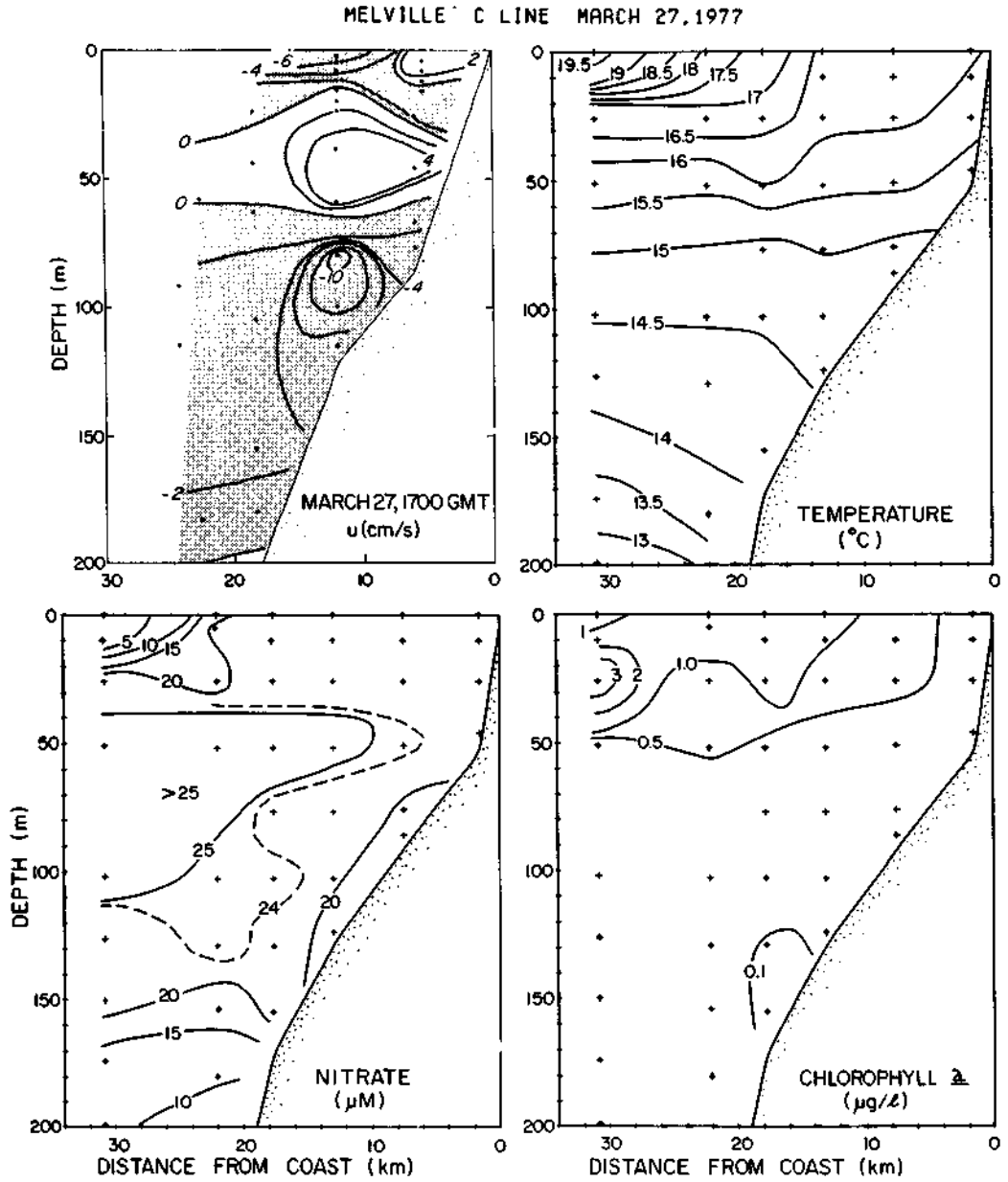

Fig. 14. Hydrographic section of March 27, 1977. Upper left, onshore velocity (cm/s). Sections are as in Fig. 11.

Although the wind event was weak and its apparent source water was of shallow (<50 m) origin, it did appear to have significant biological consequences. During period B, the phytoplankton recycling mechanism was apparently broken and the upwelling source water was not restocked. Water of unusually low phytoplankton content apparently surfaced. The immediate effect of the March 21 event was to decrease significantly near-surface chlorophyll a concentrations (Fig. 2). The mid-shelf phytoplankton population did not recover for the remainder of the observation period. The shelf-break chlorophyll a maximum remained, although the concentration was less than 1 μg/l throughout the water column within 15 km of the shore on the C line (Fig. 13). The surface chlorophyll a showed the same structure at the C line as did alongshore gradients associated with the surface cold area (Fig. 6b). Subsequently phytoplankton was depleted across the entire shelf and slope (Fig. 14). Near-surface nitrate increased slightly during the event, but

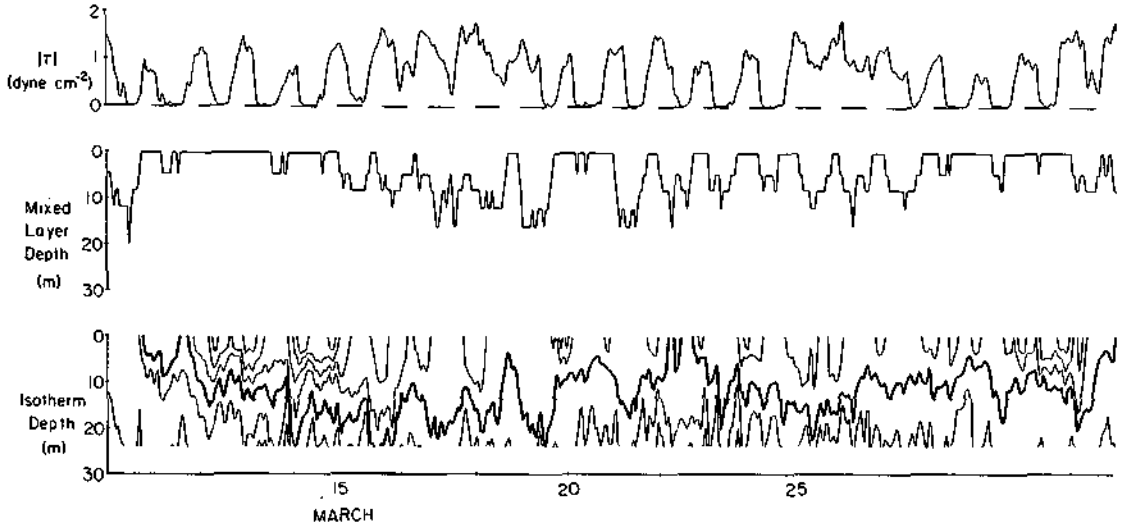

Fig. 15. Wind stress (dyne/cm^2), surface mixed layer depth (m), and isotherm depths (m) at the mid-shelf current meter mooring. Isotherm-depth contours are plotted at increments at 0.5°C, with the 16.5°C depth contour darkened. Wind and temperature data were treated with a filter having a half-power point of 2 h. A given depth is within the mixed layer if its temperature is within 0.1°C of that at 2.1-m depth.

it did not subsequently decrease, apparently because the phytoplankton growth rate was low, as suggested by low specific uptake rates for nitrogen and silicon (Fig. 18).

The second set of drogue-following biological observations began on March 22, toward the end of the upwelling event. The 4-m drogue moved initially northward, and then offshore, fairly consistent with the flow expected in a wind-driven near-surface layer (Fig. 17a). The rates of phytoplankton productivity were initially low; the specific nitrate uptake rate was less than 0.03 h^{-1} for the first 4.5 days (Fig. 17b). During the first three days, chlorophyll a, interpolated to 4 m, along the drogue path increased to only 2.8 µg/l, and the associated declines of nitrate and silica were just 5 and 6 µg/l, respectively (Fig. 17b). These low growth and uptake rates again reflect the considerable decrease in biological productivity that may have been set up by the wave passage on March 15 to

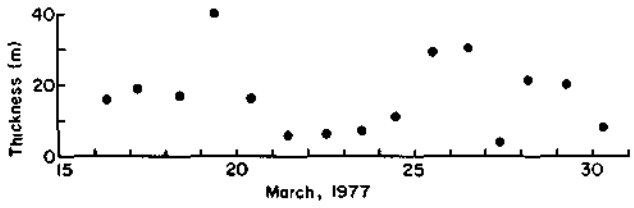

Fig. 16. Depth of the mid-shelf bottom mixed layer, derived from daily CTD observations. A given depth is within the bottom mixed layer if its temperature is within 0.1°C of the deepest measurement.

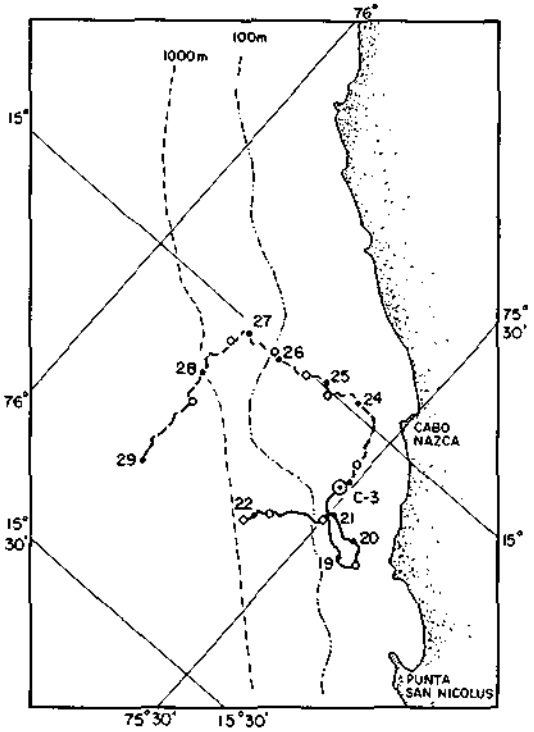

Fig. 17a. Results from the drogue-following biological observations. Drogue tracks, with solid dots representing positions at 0000 local time and open circles denoting positions of biological measurements. The first and second biologically dedicated drogue tracks are denoted by solid and dashed lines, respectively.

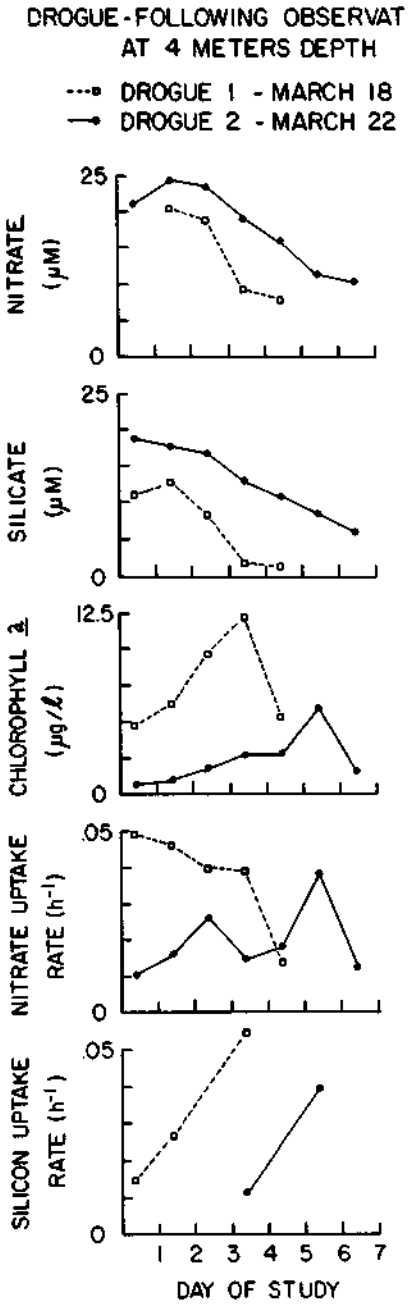

Fig. 17b. Results from the drogue-following biological observations. Time series of chemical and biological variables. Dashed line: March 18-22 drogue, solid line: March 23-28 drogue

19, as suggested above in conjunction with period B.

Period E: Weak Winds

The brief but biologically important event of March 21 was followed by a period of weak winds lasting from March 23 to 25. The onshore-offshore circulation over the shelf became relatively disorganized, with generally onshore flow above 50 m, offshore flow below 50 m, and an estimated downward vertical velocity near the coast (Fig. 3). The undercurrent was re-established, as indicated by the poleward flow below 15 m at mid-shelf. The surface mixed layer reached only moderate depths (Fig. 15). The sea-surface temperature pattern was relatively disorganized on March 23 (Fig. 8), and the central cold area was considerably smaller than on March 21. The drogues and current meters still had a tendency toward cross-isotherm flow. The physical system showed effects (e.g., no strong upwelling) ordinarily contributing to the "aging" of upwelled water, but the primary nutrients and nitrite at mid-shelf did not change significantly (Fig. 2) because of the very low phytoplankton population, hence low consumption.

Period F: Wind Event

A second strong wind event occurred during the period of March 25 to 27, but in the absence of a strong coastally trapped wave. The onshore flow pattern over the shelf suggested developed upwelling circulation and a vertical velocity estimate of as much as 33 m/day (Fig. 3), while the alongshore flow was strongly (peak > 20 cm/s) equatorward near the surface and poleward below 20 m. The 4-m drogue turned more offshore during the period (Fig. 17a). Surface temperatures were generally lower on March 25 than on March 23 (Figs 8 and 9) and a large cold area was centered just poleward of the C line. The drogue data again showed a tendency toward flow outward from the coldest part of the cold surface area. The near-surface flow at PSS turned onshore late in the event, which could be consistent with geostrophic (baroclinic) flow. Although the event

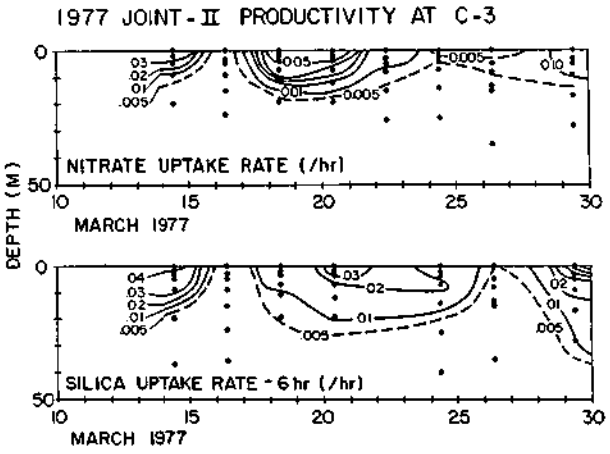

Fig. 18. Mid-shelf (C-3) time series of nitrogen and silicon specific uptake rates (h^{-1}).

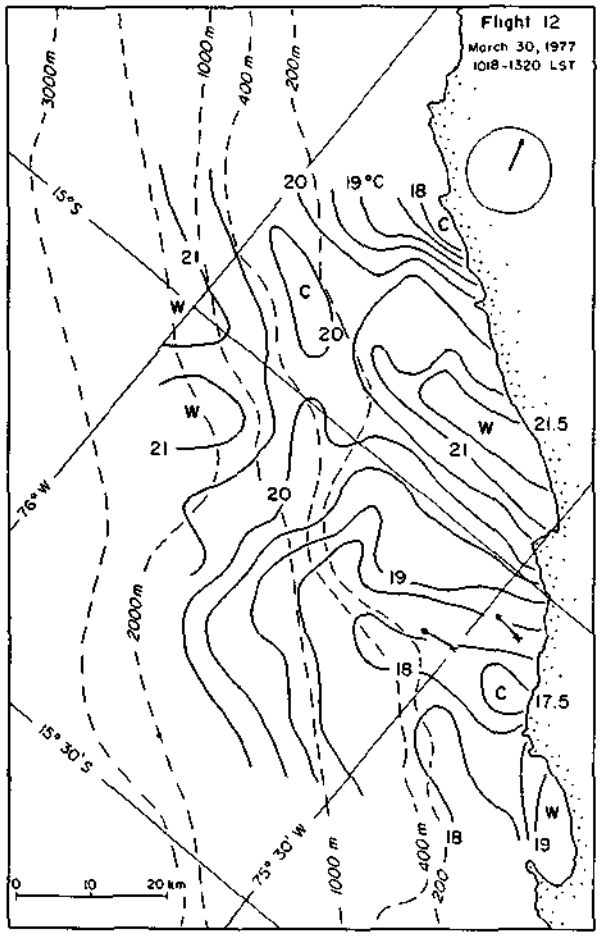

Fig. 19. Sea-surface temperature (^{o}C) from an aircraft flight near noon local time on March 30, 1977. Conventions are as in Fig. 7.

was fairly strong and had deep source waters, the best near-surface expressions of upwelling were in the low surface temperatures (<16.0^{o}C, Fig. 9). No biological or chemical consequences were observed at C-3, apparently because, in the absence of significant biological uptake, nutrient concentrations were nearly uniform with depth at mid-shelf (Fig. 2), i.e., the displaced "old" surface water had roughly the same nutrient content as the freshly upwelled water. The hydrographic section of March 27 (Fig. 14) supports this interpretation: nitrate concentrations were high (>20 μM) over most of the shelf, and chlorophyll *a* concentrations were low over the entire section. The temperature section, with its cold near-surface waters, and the cross-shelf velocity section do, however, show strong indications of upwelling.

Period G: Weak Winds

The intensive observation period ended with a phase of wind relaxation from March 27 to 30, during which the mid-shelf surface temperatures again increased (Fig. 3), the surface mixed layer was generally very shallow (Fig. 15), and the surface cold area contracted (Fig. 19). The mid-shelf onshore flow pattern became disorganized, estimated vertical velocities were variable, and the undercurrent remained strong (Fig. 3). Again, no biological "aging" of the near-surface water was evident at mid-shelf (Fig. 2); chlorophyll *a* remained low and nutrients high.

Conclusions on Temporal Variability

The period we studied may be unrepresentative. The coastally trapped wave of March 15 to 19 was the strongest that occurred during the March through May 1977 period, and the depletion of the phytoplankton stock was also unusual. Therefore, only tentative conclusions about the general patterns of variability can be drawn.

It seems that a normal sequence for upwelling, in the absence of very strong coastally trapped waves, would be the following: Within about one day (half an inertial period) of the onset of upwelling-favorable winds, upwelling of cool, nutrient-rich, phytoplankton-poor (but not totally depleted) water would be established. The vertical motion is concentrated in the nearshore area, so that the surface temperatures there become especially low, and (presumably) the nutrient concentrations high. The surface cold area would continue to enlarge as long as the upwelling continues or until it spreads to the extent that the dynamics change. During this growth phase, the surface temperature patterns are relatively regular, sharp horizontal gradients are unusual, and the near-surface flow is Ekman-like (Figs 9 and 19). The results of Brink *et al.* (1980) support these conclusions with respect to the currents. A clear statistical relation also exists between the size of the surface cold area and the alongshore wind stress: the area having sea-surface temperature less than 16.5^{o}C on the ART charts has a correlation of 0.62 (13 samples, 99% confidence) with the alongshore wind stress at San Juan, averaged for the two days prior to the ART observation. After the wind relaxes, the near-surface waters become warmer with time, primarily because of solar heating and alongshore advection. During relaxation, the sea-surface temperature and near-surface flow fields become less regular, and frontal features occur (e.g., on the northern side of the surface cold area on March 23, see Fig. 8). The tendency for the organization of the surface thermal field to vary with wind strength has also been observed in other upwelling regions (e.g., Curtin, 1979 and Barton, Huyer, and Smith, 1977).

The biological "aging" of the surface water is largely due to the growth of phytoplankton as the water moves away from the upwelling center. As the water moves offshore, its phytoplankton content should increase, provided growth exceeds losses and that nutrient supplies do not severely limit growth. As the phytoplankton grow, they

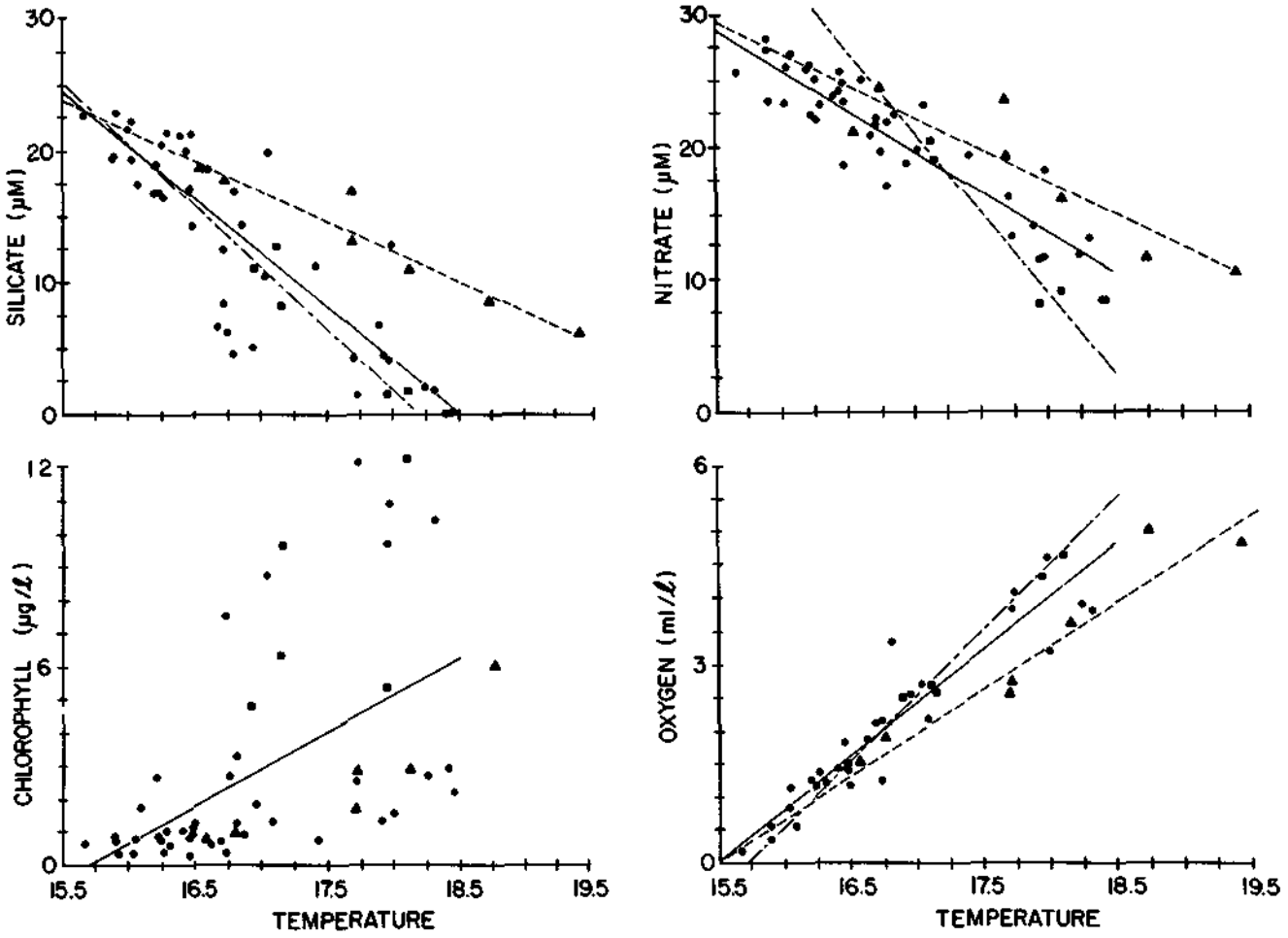

Fig. 20. Chemical variables as a function of temperature in the upper 25 m of the water column (March 12 to 30, 1977). Circles represent hydrographic data, and the solid line is the resulting linear regression equation. Squares (triangles) and the dash-dot (dashed) line are from the first (second) set of drogue-following biological observations.

consume primary nutrients in the near-surface layer, notably nitrate, phosphate, and silicate. Nitrite may increase due either to phytoplankton release or to bacterial nitrification of ammonia (Estrada and Wagensberg, 1977). Thus, as the upwelled water "ages", we expect increased phytoplankton biomass (chlorophyll *a*) and nitrite, and decreased nitrate and silicate concentrations. Losses to the phytoplankton are, however, expected. Diatoms, for example, tend to settle out of the euphotic zone, especially when nutrients become scarce. Grazing by both fish and zooplankton can also account for losses and leave increased ammonia concentrations as a by-product. Ammonia in the surface layer can usually be taken as a sign of grazing and thus of "aging" water. Horizontal advection out of the system is another potential means of removing phytoplankton. This sequence for "normal" upwelling has some support in our observations. The period March 12 to 16 seems to show the sequence fairly clearly, as did the first set of drogue-following biological observations. The physical component of this sequence appears to hold during most of the period.

The above sequence does not apply strictly throughout the March 12 to 30 period, however, because of both reduced phytoplankton concentrations and changes in the species composition, which may have been related to the passage of a coastally trapped wave. (Alternatively Smith and Barber, 1980, carried out some two-dimensional calculations that suggest that the species change of March 20 to 23 may have been due only to cross-shelf advection.) It is difficult to assess the biological impact of the waves. Over the shelf, a wave causes an alongshore velocity perturbation that is relatively depth-independent and causes large temperature fluctuations only below about

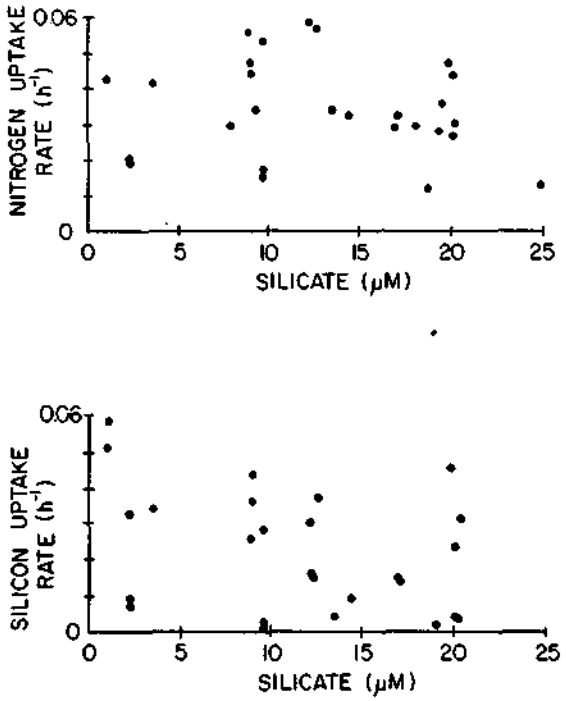

Fig. 21. Specific uptake rates at the 50 and 30% levels as a function of silica concentration (μM), March 12 to 30, 1977. a) nitrate uptake rate (h^{-1}); b) silica uptake rate (h^{-1}).

80-m depth (Brink *et al.*, 1980). Most of the upwelling source water seems to be of shallower origin (see, for example, Fig. 3), so that temperature-nutrient correlations would suggest only small perturbations in the chemical content of upwelled water associated with the waves. Apparently, then, the major direct effect that the waves could have on the biology is through alongshore advection, thus the breakdown of the hypothetical phytoplankton "reseeding" mechanism.

The Biological Surface Expression of the Upwelling Center

Maps based on observations from ships were occasionally drawn of the 15°S upwelling center during the JOINT-II observations, and these often showed chemical and biological structures analogous to that in sea-surface temperature (e.g., Fig. 6) (see also Kelley, Whitledge, and Dugdale, 1975; Boyd and Smith, 1980; Jones, 1977). The structures in the maps are not simple, and the correspondence of chemical and thermal features is not exact. Nevertheless, it is useful to explore the correlations of chemical variables with temperature.

Data from hydrographic sections and the drogue-following studies were used to construct plots of biologically-related variables vs. temperature in the upper 25 m (chosen to include the maximum depth of the surface wind-mixed layer and the euphotic zone). The observations from the drogue-following study were interpolated to 4 m, the depth of the drogue. Sea-surface temperature is taken to approximate the "age" of the upwelled water, as discussed above.

Primary nutrients decreased approximately linearly with increasing temperature. Silica (Fig. 20a) had a maximum of about 23 μM at 15.5°C and decreased to nearly zero at 18.5°C. Nitrate (Fig. 20b) and phosphate (not shown) also decreased linearly with temperature but did not intercept the temperature axis at or below 18.5°C. Thus, silicate was probably a limiting nutrient during the period, particularly at temperatures equal to or greater than 18.5°C. The depletion of silicate also suggests that diatoms were a major part of the local phytoplankton population. The distribution of chlorophyll *a* relative to temperature (Fig. 20c) is bimodal, unlike the primary nutrients or oxygen (Fig. 20d). Because of the good correlations of nutrients and oxygen with near-surface temperature, we expect that mean surface contour plots of these variables would show structure similar to that of the mean temperature plot (Fig. 1).

Differences in 4-m temperatures between the start and finish of each drogue study can be used to estimate nutrient depletion and oxygen generation with regression coefficients derived from Fig. 20. Using the Redfield, Ketchum, and Richards (1963) ratio of $\Delta O:\Delta C:\Delta N:\Delta P = -276:106:16:1$, estimates of the carbon fixed by the phytoplankton were made from the computed nutrient changes and compared with primary productivity integrated over the drogue periods using observations given by Barber *et al.* (1978) (Table 1). The direct estimates of carbon productivity, representing

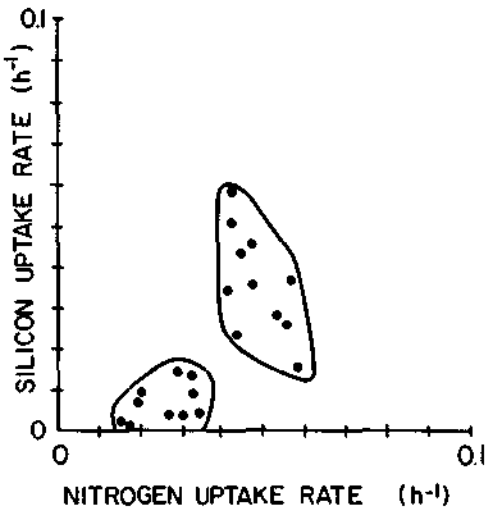

Fig. 22. Silica uptake rate (h^{-1}) vs. nitrate uptake rate (h^{-1}).

TABLE 1. Biological Rate Calculations

	Observed		Estimated from Regression		
	ΔT_{4m}	ΔC^*	ΔO	ΔN	ΔP
Drogue Study 1:					
Change along drogue	1.03°C	54.9	177	-12.9	-0.64
ΔC based on Redfield Ratio			67.8	85.3	68.2
$\frac{\text{Measured } \Delta C}{\text{Potential } \Delta C}$ (%)			81	64	80
Drogue Study 2:					
Change along drogue	2.87°C	63.9	328	-13.8	-1.11
ΔC based on Redfield Ratio			126	91.4	118
$\frac{\text{Measured } \Delta C}{\text{Potential } \Delta C}$ (%)			51	70	54

* The measured carbon production is the sum of the depth-averaged euphotic zone simulated *in situ* measurements during the drogue-following studies (Barber *et al.*, 1978). All changes, except for temperature, are in µg-at/l.

averages for the entire euphotic zone, indicate that phytoplankton uptake accounted for 50 to 80% of the changes in chemical variables.

The nutrient-temperature regression results can be used to estimate phytoplankton process rates. The approximate mean travel time for surface transport between the coast and the 18.5°C isotherm was about three days. The mean surface chlorophyll *a* concentration at position C-1 was about 1 µg/l (Fig. 10d). From the nitrate-temperature regression, the decrease in nitrate concentration between the coast and the 18.5°C isotherm was about 19 µM. Using the rule of thumb that 1 µg/l of chlorophyll is produced per 1 µM of nitrogen consumed, then total estimated chlorophyll *a* production was 19 µg/l. From the chlorophyll *a*-temperature regression, an increase to 6.2 ± 2.8 µg/l at 18.5°C can be estimated at 99% confidence. Thus the estimated mean net growth rate is about 0.4 to 0.7/day. The gross growth rate estimated from the change in nitrate is 1.0/d. Assuming no losses due to mixing, a net loss rate of 0.3 to 0.6/day is estimated. We assume the loss is due to grazing and to sinking. Grazing by large copepods (*Calanus chilensis*, *Eucalanus inermis*, and *Centropages brachiatus*) accounted for less than 5% of the daily primary production during April, 1977 (Dagg *et al.*, 1980). Sediment trap measurements by Staresinic, Rowe, and Clifford (1980) and by Staresinic (1978) show that in 1977 about 9% of the daily surface primary productivity sank from the euphotic zone. Thus, there is an observed minimum loss rate of 14% compared to our estimated 30% to 60%. Our estimated growth rate (equivalent to 1.4 doublings/day) agrees with the carbon doubling rates at depths shallower than the 15% light penetration depth, as measured by simulated *in situ* uptake studies (Barber *et al.*, 1978). Thus, the observed (Fig. 6) or inferred (from regression) scales of surface chemical structures are fairly consistent with *in situ* rates.

Uptake rates of nitrogen and silicon show no simple dependence on the concentration of silica (Fig. 21), the apparent growth-limiting nutrient. A plot of nitrogen vs. silicon uptake rates (Fig. 22) shows that the observations fall into two groups. One group has high uptake rates of both nitrogen and silicon. The second group has low nitrogen uptake rates and lower silicon uptake rates. The observations in this low-rate group fall into two categories. The first includes measurements from period A, when it seems that the low uptake rates were due primarily to low nutrient concentrations. The other observations in the low-rate group were made after March 21, when nutrient concentrations were high (Fig. 2), but flagellates represented a relatively larger fraction of the phytoplankton species composition (Dolors Blasco, personal communication). Thus the changes in nutrient uptake rates during March 12 to 30 were apparently due both to nutrient limitation and to changes in the phytoplankton species composition. The changes in uptake rates will presumably cause the chemical signature of the upwelling center to vary in its intensity. Nonetheless, the tendency for the chemical reflection of the upwelling center to mimic the thermal structure should generally obtain.

Conclusions

Our study of the upwelling center near 15°S gives a partial description of its behavior.

While ambiguity remains concerning some aspects, a few general points are quite clear. The near-surface region especially displays strong temporal variability on the diurnal time scale and longer and is extremely responsive to variations in the wind and in surface heating. Within the upwelling center, there appears to be a considerable dependence of biological and chemical variables on the physical environment. Both the biological and the physical features are strongly three-dimensional and seem to have most of their structure concentrated in the upper 50 m or less of the water column. Although the physical "horizontal plume" is a shallow feature, its biological significance is assured because the phytoplankton are generally concentrated near the surface.

Questions remain concerning the near-surface physical and biological dynamics of the upwelling center. Is the edge of the surface cold area a deformed front, or is there generally a more gradual transition between the freshly upwelled waters and the ambient surface waters? Unambiguous intense fronts have not been thoroughly documented by sub-surface observations, although surface measurements (e.g., ART charts) occasionally show sharp fronts, usually on the lateral boundaries of the cold area. Closely related to the question of fronts is the nature of the near-surface flow. To the extent that the fronts are important, near-surface flow will tend to have a thermal wind balanced component parallel to the front and a frictional component perpendicular to the front. Our observations do not allow a clear evaluation of the importance of the two factors. Another question of considerable importance, which we have not addressed, is why does the surface cold area, i.e., the apparent plume, exist, and why is the location of its coastal origin so stable? The locally intensified alongshore component of the wind stress, discussed above, will certainly contribute to this phenomenon. Also, the numerical experiments reported by Preller and O'Brien (1980) suggest that upwelling is locally intensified because of interaction of the undercurrent with nearby irregularities in the continental shelf topography. The validity of the phytoplankton "reseeding" hypothesis must be resolved. The onshore flow at depth varies strongly in the alongshore direction (Brink *et al.*, 1980), so that estimates based on data from C-line current meters do not allow a sufficient test. Yet the substantial productivity of the upwelling center (relative to its immediate surroundings) and the significant temporal variations in nutrient uptake rates suggest that there is indeed a biological concentration mechanism related to the physical regime. Future studies of regions such as this will probably require a greater concentration of resources on near-surface observations. The numerous ambiguities of this study point out a need for physical, chemical, and biological observations to define the entire spatial extent of the cold area. Temporal intensity must be adequate to document, without ambiguity, the response of the structure to its forcing functions. These constraints will probably require at least daily mapping of the surface feature and careful monitoring of the wind forcing and sub-surface variability.

Finally, one might ask whether upwelling center phenomena as we have described them here are confined to the Peruvian and perhaps California (Traganza, Nestor, and McDonald, 1980) upwelling systems, or if they are more universal. In other words, is an upwelling center simply another manifestation of the more nearly alongshore uniform dynamics found, for example, off Oregon (Holladay and O'Brien, 1975)? It is our opinion that the upwelling center near 15°S is unusual only in its relatively short (∿30 km) alongshore scale, the persistent shallowness of the poleward undercurrent, and the importance of free, coastally trapped waves. These differences do not appear to make the upwelling center near 15°S particularly anomalous.

Acknowledgements. We would like to express our appreciation to all of those scientists who made their data available for this study: Drs. R.T. Barber, L.A. Codispoti, J.J. Goering, D. Halpern, A. Huyer, and R.L. Smith. Funding for the research was provided by the International Decade of Ocean Exploration (IDOE) office of the National Science Foundation (NSF) through grants OCE 78-03380, OCE 79-22547, OCE 75-22444, OCE 77-28354, OCE 77-27735, OCE 78-03042, OCE 77-27006, and OCE 78-00611.

References

Barber, R.T., Variations in biological productivity along the coast of Peru: the 1976 dinoflagellate bloom, *Science*, in press, 1981.

Barber, R.T., S.A. Huntsman, J.E. Kogelschatz, W.O. Smith, B.H. Jones, and J.C. Paul, Carbon, chlorophyll and light extinction from JOINT-II 1976 and 1977, CUEA Data Report 49, 476 pp., 1978.

Barton, E.D., A. Huyer, and R.L. Smith, Temporal variation observed in the hydrographic regime near Cabo Corveiro in the northwest African upwelling region, February to April 1974, *Deep-Sea Research, 24*, 7-23, 1977.

Boyd, C.M. and S.L. Smith, Interaction of plankton populations in the surface waters of the Peruvian upwelling region: A study in mapping, Abstracts of the IDOE International Symposium on Coastal Upwelling, University of Southern California, Los Angeles, February 4-8, 1980, American Geophysical Union, Washington, D.C. (abstract only), 1980.

Brink, K.H., D. Halpern, and R.L. Smith, Circulation in the Peruvian upwelling system near 15°S, *Journal of Geophysical Research, 85*, 4036-4048, 1980.

Brink, K.H., R.L. Smith, and D. Halpern, A compendium of time series measurements from moored

instrumentation during the MAM 77 Phase of JOINT-II, CUEA Technical Report 45, 72 pp., 1978.
Curtin, T.B., Physical dynamics of the coastal upwelling frontal zone off Oregon, Ph.D. Dissertation, University of Miami, 338 pp., 1979.
Dagg, M., T. Cowles, T. Whitledge, S. Smith, S. Howe, and D. Judkins, Grazing and excretion by zooplankton in the Peru upwelling system during April 1977, *Deep-Sea Research, 27*, 43-59, 1980.
Dugdale, R.C., J.J. Goering, R.T. Barber, R.L. Smith, and T.T. Packard, Denitrification and hydrogen sulfide in the Peru upwelling region during 1976, *Deep-Sea Research, 24*, 601-608, 1977.
Eber, L.E., J.F.T. Saur, and O.E. Sette, Monthly mean charts: sea surface temperature North Pacific Ocean 1949-62, U.S. Bureau of Commercial Fisheries Circular, 258, 1968.
Estrada, M. and M. Wagensberg, Spectral analysis of spatial series of oceanographic parameters (fluorescence, temperature, concentrations of nitrite and of nitrate + nitrite), *Journal of Experimental Marine Biology and Ecology, 30*, 147-164, 1977.
Hafferty, A.J., L.A. Codispoti, and A. Huyer, JOINT-II R/V *Melville* Legs I, II, IV; R/V *Iselin* Leg II Bottle Data March 1977 - May 1977, Reference M78-48, University of Washington, Department of Oceanography, 779 pp., 1978.
Hafferty, A.J., D. Lowman, and L.A. Codispoti, JOINT-II *Melville* and *Iselin* bottle data sections March-May 1977, CUEA Technical Report, 38, 129 pp., 1979.
Holladay, C.G. and J.J. O'Brien, Mesoscale variability of sea surface temperatures, *Journal of Physical Oceanography, 5*, 761-772, 1975.
Huyer, A. and W.E. Gilbert, Vertical sections and mesoscale maps of temperature, salinity, and sigma-t off the coast of Peru, July to October 1976 and March to May 1977, School of Oceanography, Oregon State University, Data Report 79, 162 pp., 1979.
Johnson, W.R., P.I. Koeb, and C.N.K. Mooers, JOINT-II R/V *Columbus Iselin* Leg 1 CTD measurements off the coast of Peru March 1977, CUEA Data Report 56, 408 pp., 1979.
Jones, B.H., A spatial analysis of the autotrophic response to abiotic forcing in three upwelling ecosystems: Oregon, northwest Africa, and Peru, Ph.D. Dissertation, Duke University, 262 pp., 1977.
Kelley, J.C., T.E. Whitledge, and R.C. Dugdale, Results of sea surface mapping in the Peru upwelling system, *Limnology and Oceanography, 20*, 784-794, 1975.
Kogelschatz, J.E., J.J. MacIsaac, and N.F. Breitner, JOINT-II general productivity report R/V *Wecoma* March-May 1977, CUEA Data Report 50, 170 pp., 1980
Moody, G.L., Aircraft derived low level winds and upwelling off the Peruvian coast during March, April, and May 1977, CUEA Technical Report 56, 110 pp., 1979.
Mooers, C.N.K., C.A. Collins, and R.L. Smith, The dynamic structure of the frontal zone in the coastal upwelling region off Oregon, *Journal of Physical Oceanography, 6*, 3-21, 1976.
Preller, R. and J.J. O'Brien, The influence of bottom topography on upwelling off Peru, *Journal of Physical Oceanography, 10*, 1377-1398, 1980.
Redfield, A.C., B.H. Ketchum, and F.A. Richards, The influence of organisms on the composition of sea water, in *The Sea*, M.N. Hill (ed.), Interscience Publishers, New York, Vol. II, Chap. 2, 1963.
Ryther, J.H., D.W. Menzel, E.M. Hulburt, C.J. Lorenzen, and N. Corwin, *Anton Bruun* Reports, Scientific results of the southeast Pacific expedition, Report No. 4, Texas A&M Press, 12 pp., 1966.
Smayda, T.J., The suspension and sinking of phytoplankton in the sea, *Oceanography and Marine Biology, Annual Review, 8*, 353-414, 1970.
Smith, R.L., Poleward propagating perturbations in currents and sea level along the Peru coast, *Journal of Geophysical Research, 83*, 6083-6092, 1978.
Smith, R.L., D.B. Enfield, T.S. Hopkins, and R.D. Pillsbury, Circulation in an upwelling ecosystem: the *Pisco* cruise, *Investigacion Pesquera, 35*, 9-24, 1971.
Smith, S.L. and T.E. Whitledge, The role of zooplankton in the regeneration of nitrogen in a coastal upwelling system off northwest Africa, *Deep-Sea Research, 24*, 49-56, 1977.
Smith, W.O., Jr., and R.T. Barber, Circulation, sinking, and vertical migration as determinants of phytoplankton success in the upwelling center at 15°S, *This Volume*, 1980.
Staresinic, N., The vertical flux of particulate organic matter in the Peru coastal upwelling with a free-drifting sediment trap, Ph.D. Dissertation, Woods Hole Oceanographic Institution and Massachusetts Institute of Technology, 255 pp., 1978.
Staresinic, N., G.T. Rowe, and C.H. Clifford, The vertical flux of particulate organic matter in the Peru coastal upwelling region, Abstracts of the IDOE International Symposium on Coastal Upwelling, University of Southern California, Los Angeles, February 4-8, 1980, American Geophysical Union, Washington, D.C. (Abstract only), 1980.
Stevenson, M.R., Measurement of currents in a coastal upwelling zone with parachute drogues, *Exposure, 2*, 8-11, 1974.
Stevenson, M.R., R. Garvine, and B. Wyatt, Lagrangian measurements in a coastal upwelling zone off Oregon, *Journal of Physical Oceanography, 4*, 321-336, 1974.
Stuart, D.W. and J.J. Bates, Aircraft sea surface temperature data--JOINT-II 1977, CUEA Data Report 42, 39 pp., 1977.
Traganza, E.D., D.A. Nestor, and A.K. McDonald,

Satellite observations of a nutrient upwelling off the coast of California, *Journal of Geophysical Research, 85*, 4101-4106, 1980.

Van Leer, J.C. and A.E. Ross, Velocity and temperature data observed by Cyclosonde during JOINT-II off the coast of Peru, Rosenstiel School of Marine and Atmospheric Sciences Data Report DR 7902, University of Miami, 34 pp., 1979.

Walsh, J.J., J.C. Kelley, R.C. Dugdale, and B.W. Frost, Gross features of the Peruvian upwelling system with special reference to possible diel variation, *Investigacion Pesquera, 35*, 25-42, 1971.

Zuta, S., T. Rivera, and A. Bustamante, Hydrologic aspects of the main upwelling areas off Peru, in *Upwelling Ecosystems*, pp. 235-257, R. Boje and M. Tomczak (eds.), Springer-Verlag, Berlin, 303 pp., 1978.